HHS Public Access

Author manuscript

Oncogene. Author manuscript; available in PMC 2020 June 09.

Published in final edited form as:

Oncogene. 2020 March ; 39(10): 2156–2169. doi:10.1038/s41388-019-1134-6.

Integrin α6 signaling induces STAT3-TET3-mediated hydroxymethylation of genes critical for maintenance of glioma stem cells

Andreas Herrmann[#1,5], **Christoph Lahtz**[#1,5], **Jieun Song**[#1], **Maryam Aftabizadeh**[1], **Gregory A. Cherryholmes**[1], **Hong Xin**[1], **Tomasz Adamus**[1,5], **Heehyoung Lee**[1], **David Grunert**[1], **Brian Armstrong**[2], **Peiguo Chu**[3], **Christine Brown**[4], **Michael Lim**[6], **Stephen Forman**[4], **Hua Yu**[1]

[1]Department of Immuno-Oncology, Beckman Research Institute at City of Hope Comprehensive Cancer Center, Duarte, CA 91010, USA

[2]Department of Neuroscience, Beckman Research Institute at City of Hope Comprehensive Cancer Center, Duarte, CA 91010, USA

[3]Department of Pathology, City of Hope Comprehensive Cancer Center, Duarte, CA 91010, USA

[4]Department of Hematology and Hematopoietic Cell Transplantation, City of Hope Comprehensive Cancer Center, Duarte, CA 91010, USA

[5]Sorrento Therapeutics, San Diego, CA 92121

[6]Department of Neurosurgery, Johns Hopkins University, Baltimore, MD 21287

[#] These authors contributed equally to this work.

Abstract

Both the extracellular matrix (ECM) and DNA epigenetic regulation are critical for maintaining stem cell phenotype and cancer progression. Whether and how ECM regulates epigenetic alterations to influence cancer stem cells (CSCs) remain to be explored. Here we report that ECM through laminin-integrin α6 upregulates ten-eleven translocation enzyme 3 (TET3) dioxygenase. TET3 in turn mediates DNA cytosine 5'-hydroxymethylation (5hmC) and upregulates genes critical for maintenance of glioma stem cells (GSCs). Activating integrin α6-FAK pathway increases STAT3 activity, TET3 expression and 5hmC levels in GSCs. Moreover, targeting STAT3 disrupts integrin α6-FAK signaling and inhibits $TET3^{+}$ GSC maturation *in vivo*. STAT3 directly regulates TET3 expression and the two proteins are co-localized with 5hmC in GSC clusters. 5hmC is upregulated by STAT3 at the promoters of several tumorigenic genes, including c-Myc, known to be critical for GSCs. *In vivo* silencing of TET3 in GSC-enriched tumors reduces 5hmC accumulation and expression of the GSC critical genes, leading to tumor growth inhibition. TET3

Correspondence: aherrmann@sorrentotherapeutics.com; hyu@coh.org.

Conflict of interest

No potential conflicts of interest were disclosed by the authors.

Compliance with ethical standards

Supplementary information is available at Oncogene's website.

expression and 5hmC accumulation also co-segregate with integrin α6 in patient malignant glioma. Thus, ECM- integrin α6-STAT3-TET3 axis regulates hydroxymethylation of genes important for GSCs, thereby increasing GSC tumorigenicity and resistance to therapies.

Introduction

Glioblastoma (GBM) is the most lethal brain tumor with few if any effective therapeutics. Although many lines of experimental evidence suggest that CSCs are, too a large degree, culprits for the failure of therapies for GBM patients, further identification of pathways/targets is critical for improvement of therapeutic outcomes.

The ECM consisting of a complex network of macromolecules is a major component of the niche critical for regulating stem cell behavior. The ECM is usually dysregulated in cancer and is critical for promoting cancer metastasis [1–6]. In addition to tumor metastasis, ECM also regulates stem cell differentiation and functions [7]. Integrins are among the best characterized cell receptors on stem cells that interact with ECM [1, 3], thereby connecting the intracellular cytoskeleton with the ECM. Insoluble adhesive cues, such as ECM protein laminin sensed by integrins, can transduce into signals that regulate stem cell differentiation and fates. One of the best examples illustrating the importance of integrin signaling in promoting CSCs is the finding that integrin α6 is critical for GSC proliferation, self-renewal and tumor formation capacity of GSCs [8]. Nevertheless, the detailed molecular mechanism underlying integrin α6-induced GSC tumorigenicity remains elusive.

A critical role of STAT3 in maintaining the cancer stem phenotype has been shown [9–11]. However, STAT3 is also upregulated in non-stem tumor cells. What might enable STAT3 to have unique role in CSCs needs to be explored. Relevant to the questions, GSCs have higher expression of c-Myc, which is required for GSC maintenance as well as survival, and also survivin and Bcl_{XL}, which endow GSC with increased survival potential, to maintain CSC phenotype and survival [12–14]. The question remains what might propel higher expression of these pro-CSC genes. Is ECM/integrin- α6 pathway critical for upregulating the pro-CSC genes? And if so, what is the pathway and mechanism by which integrin α6 drives GSC phenotype/survival.

Ten-eleven translocation enzymes, TET dioxygenases, are critical for gene promoter conversion from 5mC to 5hmC, thereby favoring gene demethylation [15–17]. Although TET proteins are shown to play a tumor suppressor functions, the findings remain highly contextual [18–24]. In hematopoietic malignancies, TET1 has been found to be a tumor suppressor as well as tumor-promoter [21, 22]. TET3 was recently shown to inhibit GSCs, mainly in the context of nuclear receptor TLX [20]. High levels of 5hmC have been associated with survival for glioma patients [23]. In stark contrast, 5hmC is critical for glioblastomagenesis in proneural glioblastoma [24]. Additionally, a critical role of TET dioxygenases in regulating embryonic stem cells has been described [25]. Nevertheless, whether TET dioxygenase activity may contribute to epigenetic regulation to control CSCs phenotype and/or increase their tumorigenicity requires in depth investigation. In the current study, using highly aggressive human GSC cells, both *in vitro* and *in vivo*, we have identified that laminin-integrin α6-STAT3 pathway drives GSCs through TET3-mediated

hydroxymethylation of genes critical for GSC maintenance and survival. Moreover, we show that TET3 expression and 5hmC accumulation co-segregate with integrin α6 in GBM.

Results

TET3 promotes 5hmC accumulation and GSCs

Although an important role of TET dioxygenases in embryonic stem cells is known [25–27], whether they are critical for CSC maintenance in tumors remains to be further investigated. The human glioma cells isolated as stem-like cells (GSC008, GSC009, GSC030, and GSC106) are highly tumorigenic, display high STAT3 activity and ready to form spheres [28, 29]. We therefore compared the expression levels of TET enzymes in these human glioma stem-like cells cultured under conditions to enable either sphere formation (GSC) or differentiation (non-stem cells). We show that compared to non-stem human glioma cells, the patient derived primary GSCs expressed considerably higher levels of TET3 protein (Fig. 1A). We assessed expression of TET enzymes in the primary GSCs compared to differentiated non-stem counterparts, only TET3 is consistently upregulated in all 4 GSCs (Supplementary Fig. S1A), while TET1 and TET2 protein expression was barely detectable in GSCs (Supplementary Fig. S1B).

To assess whether TET3 contributes to GSC maintenance and sphere formation characteristic for GSCs, we silenced *TET3* in the primary patient-derived GSC lines, which significantly reduced their ability of GSC sphere formation (Fig. 1B). By contrast, overexpressing *TET3* in those GSC lines increased their ability of GSC sphere formation (Fig. 1C). Moreover, silencing *TET3* expression diminished self-renewal capacity of patient-derived primary GSCs as shown by limited dilution assay (LDA), which assesses the frequency of repopulation (Fig. 1D) [30].

Because DNA cytosine 5'-hydroxymethylation (5hmC) is a product of TET3 enzyme activity, we hypothesize that 5hmC becomes a substrate for deamination in GSCs [31]. Direct comparison of DNA cytosine modifications using flow cytometric analysis showed increased levels of DNA hydroxymethylation (5hmC) and considerably elevated levels of its deamination product 5'-hydroxymethyluracil (5hmU) in GSCs (Fig. 1E). Moreover, levels of 5hmC in GSCs were significantly higher than those in their non-stem counterparts (Fig. 1F). Confocal imaging analysis following immunohistochemistry of human glioma tumor tissues indicated that 5hmC was restricted to cells positive for CSC markers, such as MSI-1, SOX2 and activated STAT3 (Fig. 1G).

Our results so far suggest that TET3 is upregulated in GSCs over their non-stem tumor cell counterparts (Fig. 1).

Integrin α6/FAK critical for 5hmC accumulation

The question remains what is unique about GSCs that allows elevated expression of TET3. Integrin α6, the cognate receptor for the integral ECM protein laminin, is upregulated selectively in GSCs, and critical for GSC maintenance [8]. However, the mechanisms by which ECM/integrin α6 drives GSCs remains to be further elucidated. To assess whether integrin α6 driven GSCs requires TET3/5hmC, we compared differentiated non-stem glioma

cells with their GSC counterparts. Our results showed that integrin α6 protein expression was considerably elevated in patient-derived human GSCs (Fig. 2A and Supplementary Fig. S2), confirming findings from a previous report [8]. We next assessed induction of TET3 protein expression upon ectopic exposure of GSCs to components of the fibrous ECM, including laminin. Laminin, together with collagen and fibronectin interlaced with embedding non-fibrous proteoglycans, assembles the fibrillar networks of the ECM [2, 7]. We incubated single-cell GSC suspension in collagen, fibronectin, heparan sulfate proteoglycans (HSPG) or laminin. TET3 protein expression was robustly induced by laminin as assessed by flow cytometry and Western blotting (Fig. 2B, upper panels). Moreover, culturing a single-cell suspension of GSCs with laminin resulted in sphere formation characteristic of CSCs in 3D culture (Fig. 2B, lower panels). The GSC spheres were not detectable in collagen, fibronectin or HSPG treated cultures (Fig. 2B, lower panels). Furthermore, treating GSCs with laminin induced FAK and STAT3 activation as well as TET3 expression, which was accompanied by an increase in 5hmC modification (Fig. 2C). Conversely, inhibiting FAK activity by FAK inhibitor blocked STAT3 activation and TET3 expression, as well as 5hmC production (Fig. 2D), which was associated with the loss of GSC sphere integrity (Supplementary Fig. S3A). The cytohistochemistry and Western blotting results confirmed activation of FAK and STAT3 signaling was associated with increased protein expression of TET3 upon laminin treatment (Supplementary Fig. S3B). Furthermore, activation of FAK and STAT3 signaling was inhibited by silencing intergrin α6 or TET3 expression (Fig. 2E and 2F). Moreover, STAT3 knockdown resulted in considerably reduced TET3 expression in GSC-like cells *in vivo* (Fig. 2G).

We further assessed STAT3 transcriptional control of TET3 expression. Chromatin immunoprecipitation showed that STAT3 binds to the TET3 promoter in the human primary GSCs (Fig. 2H).

STAT3/TET3 forms complex with DNA 5mC

We next assessed how STAT3/TET3 might epigenetically regulate GSCs. We found pSTAT3/TET3 overexpression and co-localization in various human primary GSC lines derived from patient tumor samples (Fig. 3A). Immunoprecipitation pull-down experiments with either anti-STAT3 or anti-TET3 antibodies showed a robust complex formation between STAT3 and TET3 (Fig. 3B). The interaction between STAT3 and TET3 proteins was robust in laminin treated GSCs, while silencing integrin α6 inhibited STAT3-TET3 complex formation (Fig. 3C). Moreover, confocal STED microscopy revealed that pSTAT3 is co-localized in confined subnuclear domains with TET3 and its product 5hmC in patient glioma tumor tissues (Fig. 3D and Supplementary Fig. S4A–C). Furthermore, STAT3 exhibited a higher binding affinity to a methylated, compared to an unmethylated, STAT3-binding DNA oligo as analyzed by EMSA (Supplementary Fig. S4D). We were able to further demonstrate that TET3 was found in the same DNA-binding complex recognizing a methylated STAT3-consensus binding site, as assessed by an oligo-pull-down assay (Fig. 3E). These results suggest the formation of a complex of STAT3/TET3 with DNA 5mC, which could enable conversion of 5mC to 5hmC.

Targeting STAT3 and TET3 decreases promoter hydroxymethylation of GSC associated genes and GSCs

We next tested how RNAi-based STAT3 silencing would affect DNA hydroxymethylation of promoters of genes critical for GSC maintenance and key characteristics such as survival and proliferation that enable them to resist therapies. 5-hydroxymethylation of *c-Myc*, *Survivin*, and Bcl_{XL} promoters was readily detectable in GSC-like cells. Upon STAT3 knockdown, 5-hydroxymethylation of *c-Myc*, *Survivin*, and Bcl_{XL} promoters was markedly decreased as demonstrated by PCR using primers flanking the STAT3 DNA-binding site (Fig. 4A).

This prompted us to silence TET3 in human primary GSCs *in vivo*. We implanted human primary GSCs, GSC030 and GSC106 stably expressing inducible TET3 shRNAs into NOD/scid/IL2R$^{-/-}$ (NSG) mice, and TET3 knock-down significantly prolonged mouse survival (Fig. 4B). In addition to anti-GSC effects by CpG-*STAT3siRNA in vivo* as we have reported [9], treatment with CpG-*TET3siRNAs* as well as a combination of both resulted in significantly tumor growth delay of human primary GSC tumors when compared to a control CpG-siRNA conjugate (Fig. 4C). Furthermore, analyzing gDNA prepared from the tumor tissues indicated that the *c-Myc* promoter underwent significant 5-hydroxymethylation reduction *in vivo* upon silencing either TET3 or STAT3, or both via CpG-siRNA approach (Fig. 4D). Moreover, silencing TET3, STAT3, or both combined via CpG-siRNA significantly reduced global 5-hydroxymethylation *in vivo* (Fig. 5A, 5B and Supplementary Fig. S5). Moreover, silencing TET3, STAT3, or both combined, significantly downregulated integrin α6/FAK/STAT3/TET3, decreased 5hmC accumulation and significantly reduced the expression of c-Myc, Bcl_{XL}, and Survivin at protein level (Fig. 5C and 5D).

TET3 expression and 5hmC accumulation co-segregate with integrin α6 in GBM

Several studies indicated a correlation between 5hmC overall levels and glioma disease stages and patient survival [23, 32], the status of 5mhC in GSCs within patient tumors has not been reported. To assess the relationship between TET3–5hmC and GSCs in patient glioma, 19 patient glioma tumor sections, spanning grades 2/3 and GBM, were analyzed for the association of integrin α6 expression with either TET3 protein expression or 5hmC accumulation (Fig. 6A). The majority of cases analyzed show that the expression level of integrin α6 was associated with 5hmC accumulation, although 5hmC was also detected in the absence of integrin α6 expression (Fig. 6A and 6B, upper panels). Correspondingly, integrin α6 expression was shown to be accompanied by TET3 protein expression in the majority of patient samples. Notably, TET3 expression in the absence of integrin α6 expression was not observed (Fig. 6A and 6B, lower panels). Significantly, the association of integrin α6 expression with TET3 and 5hmC was found to be confined to high grade GBM specimens (Fig. 6C).

Discussion

Previous studies have emphasized the importance of specialized niches, including perivascular and hypoxic regions, in anchoring GSCs in the tumor microenvironment, which

is supported by many growth factors and cytokines, such as HIF1α and IL-6 [10, 33]. More recent studies have also suggested the critical role of ECM, via laminin-integrin α6 axis, in driving GSCs [8]. Nevertheless, the critical events downstream of integrin α6 in promoting GSC phenotype and ability to survive/proliferate thereby resisting both radiation and chemo-therapies remain to be explored. This study reveals that integrin α6, whose expression is characteristic of GSCs, signals through STAT3-TET3 to promote GSCs.

Although much is appreciated about the role of epigenetic regulation in guarding stem cell from differentiation [34–38], relatively little is known whether and how epigenetic reprogramming might promote CSC maintenance and phenotype. Nevertheless, a recent report suggested an important role of TET3 in inhibiting GSCs, mainly in the context of nuclear receptor TLX [20]. While knocking down TET3 was also shown to inhibit GSCs, the cell lines used in the two studies may differ. Our findings that TET3 and 5hmC co-segregate with integrin α6 are also confirmed in patient malignant gliomas. That different lineages of glioblastoma cells display opposing levels of 5hmC in terms of tumorigenicity has been reported [24, 32, 39, 40]. Granted biology is usually contextual, it is of high scientific interest to identify the causes of the discrepancies between our current study and the one by Cui et al [20] in terms of TET3's role in GSCs.

Nevertheless, more recent studies have suggested oncogenic roles of TET enzymes and their potential to epigenetically reprogram pluripotent cell populations. Our findings are support the recent study [39] showing that TET enzymes play important roles in hypoxia mediated induction of pluripotency in gliomas. The study showed that expression of OCT4 and NANOG, which have known to be important for stem cell properties, increased after induction of TET1 and TET3 by hypoxia in glioma cell line. More recent studies have also suggested STAT/TET1 axis as a therapeutic target for acute myeloid leukemia (AML) [22, 40]. TET1 blockade using a chemical compound suppressed AML progression *in vivo*. Our data show that GSCs undergo epigenetic editing triggered by ECM/laminin, allowing elevated expression of genes important for maintenance of GSCs by hydroxymethylation.

The transcription factor STAT3 represents a central node in connecting ECM with hydroxymethylation of genes important for GSC maintenance and survival. We have delineated an ECM-intracellular signaling axis—laminin/integrin α6-FAK-STAT3-TET3–5hmC—in upregulating expression of genes critical for GSC maintenance, survival and proliferation, thus promoting GSC phenotype and resistance to therapies. STAT3 also facilitates 5hmC conversion by interaction with TET3. Our *in vivo* studies also suggest that TET3 can be a target for reducing GSCs thereby reversing drug resistance often associated with an increase in CSCs. The importance of TET3 and 5hmC in GSCs in GBM has also been validated in patient tumors. Taken together, our data indicate a novel and distinct ECM-regulated intracellular signaling pathway that promotes GSC phenotype and underlies GSC strong survival via DNA epigenetic regulation.

Materials and Methods

Cell lines and tissue

Previously characterized and published human primary, low-passage GSC cell lines, GSC008, GSC009, GSC030, and GSC106 [28, 29] (kindly provided by Dr. Christine Brown, City of Hope, in 2018) were cultured in GSC medium [DMEM/F12 (1:1) supplemented with HEPES (Gibco), B-27 (Invitrogen), Heparin-sodium (Sagent), antibiotics-antimycotics (Gibco), 20 ng/ml FGFb, 20 ng/ml EGF (Peprotech), 20 ng/ml leukemia inhibitory factor and GlutaMAX (Gibco)]. Cell culture was performed in ultra-low adhesion plates (Corning). Primary human GSC-like lines were subcultured using Accutase (Innovative Cell Technologies, Inc) to break up sphere clusters. Only the low passages cell lines were used in the study. For differentiation of GSC cell lines, single cell suspensions were washed with HBSS, than cultured in differentiation medium [DMEM/F12 (1:1) supplemented with 7% fetal bovine serum, HEPES (Gibco), GlutaMAX (Gibco), and antibiotics-antimycotics (Gibco)] for 7 – 14 days. For generation of lentivirus expressing shRNAs, non-targeting RNA (ntRNA) (GCGCGATAGCGCTAATAATTT), shSTAT3 (CCTGAGTTGAATTATCAGCTT), shTET3 #1 (GAACCTTCTCTTGCGCTATTT), shTET3 #2 (ACTCCTACCACTCCTACTATG), or shITGA6 (CGGATCGAGTTTGATAACGAT) were cloned into Tet-pLKO-mCherry vector. For TET3 overexpression, lentiviral vector expressing full length human TET3 cDNA and puromycin resistance gene was purchased from Applied Biological Materials Inc. Lentiviruses were produced in 293T cells using cloned or purchased vectors, and GSC030 or GSC106 cells were infected with shRNA or TET3 expressing lentiviruses. The mCherry/shRNA expressing cells were sorted by flow cytometry, and TET3 overexpressing cells were selected by puromycin treatment. TET3 or STAT3 shRNA knock-down was induced by adding 5 μg/ml of doxycycline to complete growth media. All cell lines were tested for *Mycoplasma* every 6 months using MycoAlert™ PLUS mycoplasma detection kit (Lonza, last tested in December 2018). Human brain tumor tissue sections embedded in paraffin were obtained from pathology core at City of Hope and Biomax (HuCAT018, HuCAT019).

Tumor growth kinetics *in vivo* and orthotopic brain tumor model

Mice were housed in a pathogen free animal facility at the Beckman Research Institute at the City of Hope National Medical Center, and animal study was carried out in accordance with the established institutional guidance and approved protocols from Institutional Animal Care and Use Committee at the Beckman Research Institute of City of Hope National Medical Center in compliance with NIH guidelines. Both male and female mice were used for the study, and the studies were not blinded. For tumor growth kinetics *in vivo*, athymic nude mice were purchased from the Jackson Laboratories, and 2.5 X 10^6 GSC030 cells were engrafted subcutaneously to the mice supported by phenol-red free Matrigel (Corning) with phenol-red free RPMI1680 media at a 1:1 ratio. The mice were randomly assigned to be in the groups, and each group had four mice. Tumor bearing male mice were treated locally with 782.5 pmol/dose of CpG-*luciferase*-siRNA, CpG-*STAT3*siRNA [9], or CpG-*TET3*siRNA (equimolar mix of 3 CpG-siRNA conjugates comprising: sense-strand 1: 5’-GCAGACCAGUGUAACAACATT-3’, antisense-strand 1: 5’-GGTGCATCGATGCAGGGGGG-linker-UGUUGUUACACUGGUCUGCTT-3’; sense-

strand 2: 5'-GAAGCAGAGUCUUUAAUGATT-3', antisense-strand 2: 5'-GGTGCATCGATGCAGGGGGG-linker-UCAUUAAAGACUCUGCUUCTT-3'; sense-strand 3: 5'-GGAAAGCCAUUAGAUGAAATT-3', antisense-strand 3: 5'-GGTGCATCGATGCAGGGGGG-linker-UUUCAUCUAAUGGCUUUCCTT-3', *TET3siRNA* sequences were adapted from Santa Cruz, sc-94636) every other day, and volumes of tumors were measured every other day. For orthotopic mouse model, female NOD/scid/IL2R$^{-/-}$ (NSG) mice were anesthetized with ketamine (100 mg/kg) and xylazine (20 mg/kg) mixture and 1 X 10^5 GSC030 or GSC106 cells stably expressing non-targeting shRNA or *TET3* shRNAs were engrafted into the striatum. One week after tumor cell injection, the mice were started to treat with doxycycline water (2 mg/ml) to induce shRNA expression. The mice were euthanized when they showed a neurological symptom of brain tumor and mouse survival was analyzed by plotting Kaplan-Meier survival curves using GraphPad Prism 7.0 software.

Immunoprecipitation, oligo-pull-down, and western blotting

Whole cell lysates were prepared using RIPA lysis buffer containing 50 mM Tris-HCl, pH7.4, 150 mM NaCl, 1 mM EDTA pH8.0, 0.5% NP-40, 1 mM NaF, 15% glycerol, and 20 mM β-glycerophosphate. Protease inhibitor cocktail was added freshly to the lysis buffer (miniComplete, Roche). For immunoprecipitation, antibodies were coupled to ProteinG Agarose beads (Invitrogen) prior to adding them to the cell lysates. Precipitation was performed overnight with shaking at 4°C. Then complexes were carefully washed and proteins were electrophoretically separated by SDS-PAGE followed by Western blot detection using antibodies raised against TET1 (ThermoFisher, MA5–16312), TET2 (ThermoFisher, PA5–35847), TET3 (abcam, ab135033 and ThermoFisher, PA5–31860), integrin α6 (Santa Cruz, sc-13542), STAT3 (Santa Cruz, sc-482 and Cell Signaling, 9139), pSTAT3 (Cell Signaling, 9145), pFAK (Cell Signaling, 8556) and β-actin (Sigma, A1978). STAT3-sensitive oligo-pull-down was performed using 2 μg biotinylated SIE ds-oligo (SIE-wt: 5'-AGCTTCATTTCCCGTAAATCCCTAAGCT-3'; SIE-5mC: 5'-AGCTTCATTTCCC^{m}GTAAATCCCTAAGCT-3') which was incubated with 400 μg [protein] nuclear extract of cells in 500 μl binding buffer comprising 12 mM HEPES (pH7.9), 12% glycerol, 4 mM Tris/HCl (pH7.9), 150 mM KCl, 1 mM EDTA and freshly added 1 mM DTT, 0.1 μg/μl poly (dI:dC), 0.5 μg/μl BSA for up to 2 h at RT. Add sample to streptavidin magnetic beads (SMB) suspension of 50 μl SMB/sample prewashed thrice with binding buffer and cleared in a magnetic stand, and incubate for oligo-pull-down by SMB for 2 h at RT with rocking. Precipitate was resuspended in 4X Laemmli buffer subsequent to supernatant clearance in a magnetic stand and resolved on SDS-PAGE prior to membrane transfer and immunodetection.

Sphere formation of cell lines and treatments

For sphere formation, single cell suspensions were plated in ultra-low adhesion plates (Corning) with GSC medium. Spherical cell clusters were treated every day with 500 pmol/ml of CpG-siRNA conjugates or were cultured with 5 μg/ml of doxycycline for shRNA induction. Number of spheres was counted every other day.

Limiting-dilution assay (LDA)

Cells were cultured for at least 10 days in sphere forming medium. Prior to sphere assays, cells were placed into single cell suspension. Cultures free of clumping and being of ≥ 90% viability were used. Cells were serially diluted from 500 to 2 cells per well into 96-well and cultured in GSC medium, and fresh EGF and bFGF (PeproTech) were added every other days. The cells were cultured with 5 μg/ml of doxycycline for shRNA induction. Subsequently, cultures were analyzed for spheres in each well. Data were analyzed using the Extreme Limiting Dilution Algorithm (ELDA) [41].

Flow cytometry

Antibodies for flow cytometry were purchased from Cell Signaling Technologies (pY397FAK #3283, pPaxilin #2541), abcam (TET3 #ab135033, 5hmU #ab19735), Novus Biologicals (laminin #NB300–144), Active Motif (5mC #39649) or BD Biosciences (pSTAT3 #557815). Secondary antibodies used were coupled to either Alexa Fluor 647 or Alexa Fluor 488 (Invitrogen) diluted up to 1:4,000 in PBS/1% BSA staining buffer. For blocking FAK activity, GSC cell lines were treated with 10 μM FAK inhibitor (Santa Cruz #sc-203950). Intracellular staining was performed after fixation of single cell suspensions with 2% paraformaldehyde and permeabilization with ice-cold 100% methanol, blocked with PBS/1% BSA for 1h at 4°C, and stained with an antibody diluted at 1:50 in PBS/1% BSA for 30 – 45 min at room temperature. Detection of DNA modification was performed upon RNA digestion using RNase A at 40 μg/ml for 10 min at 37°C prior to blocking procedure. Stained single cell suspensions were analyzed using an AccuriC6 cytometer (BD Biosciences), followed by FlowJo 7.6.1 analysis.

Imaging

Indirect immunofluorescence on frozen tissue sections or paraffin embedded tissue specimen was carried out as previously described [42]. Briefly, after deparaffinization and antigen retrieval at low pH citrate buffer (Vector), tissue microsections were fixed with 2% paraformaldehyde, followed by permeabilization with ice-cold 100% methanol, treated with signal enhancer (Image-iT, Invitrogen) for 30 min, blocked with PBS containing 10% goat serum and 2.5% mouse serum (Sigma) for 1h at room temperature, and stained with a 1:50 dilution of the primary antibody (TET3 #ab135033, MSI-1 #ab21628, SOX2 #ab59776, antibodies were obtained from abcam; integrin α6 #sc-13542 and pSTAT3 #sc-7993 antibodies were purchased from Santa Cruz; pY397FAK #3283 was obtained from Cell Signaling Technologies; anti-5mC #39649, 5hmC #39769, 5caC #61225, 5fc #61223 were purchased from Active Motif and 5hmU #ab19735 was from abcam) in PBS/sera overnight at 4°C. After washing with PBS, secondary antibodies were diluted 1:100 in PBS/sera containing 100 ng/ml Hoechst33342 (Invitrogen). After final washing with PBS, specimens were mounted with Mowiol (Calbiochem).

Indirect immunofluorescence on cultured cells was carried out as described previously [42]. Confocal analysis was performed using LSM510 Meta or LSM700 (Zeiss). Ultra-resolution imaging for detection of distinct distribution of nuclear pSTAT3 was performed using confocal STED microscopy (kindly supported by Laurent Bentolila, at the Advanced Light

Microscopy/Spectroscopy Laboratory Light Microscopy Core facility of the UCLA, USA, using a Leica SP5 MP-STED microscope).

Intravital multiphoton imaging was performed as previously described [42]. Blood vasculature of the brain was stained by systemic injection of 100 μg dextran-rhodamine (Invitrogen) diluted in sterile HBSS (Gibco). Fibrous ECM emission is given by second harmonic generation autofluorescence. We used an Ultima 2photon microscope for IVMPM analysis (Prairie Technologies). Acquired Z-stacks were reconstructed to full 3D view using Amira software (Visualization Sciences Group).

Hydroxymethylation (5hmC) detection

Hydroxymethylation of oncogene promoters was assessed using the EpiMark® 5hmC and 5mC Analysis Kit aobtained from New England Biolabs according to the manufacturer's instructions. Briefly, gDNA isolated by phenol/chloroform extraction was modified using T4 b-glucosyltransferase and UDP-glucose resulting in glucosylation of 5hmC (5ghmC) where 5hmC glucosylation is thought to protect cleavage of hydroxymethylated gDNA by distinct restriction enzyme MspI. Once enzymatic digestion is completed, levels of hydroxymethylation of oncogene promoters was assessed by PCR based amplification of digestion products focusing on oncogene promoter regions bearing STAT3 binding sites. STAT3 binding site flanking PCR primer pairs were designed for c-Myc, Bcl_{XL} and survivin promoter: *Birc5*-1fwd: 5'-TCAAATCTGGCGGTTAATGG-3', *Birc5*-1rev: 5'-TCAAGTGATGCTCCTGCCTA-3'; *Birc5*-2fwd: 5'-CTCGATGGGGACAAAGCA-3', *Birc5*-2rev: 5'-AGAACTGGCCCTTCTTGGAG; *CMYC*-1fwd: 5'-AGAAGCCCTGCCCTTCTC-3', *CMYC*-1rev: 5'-TGAGTCTCCTCCCCACCTT-3'; *CMYC*-2fwd: 5'-GCTGCTATGGGCAAAGTTTC-3', *CMYC*-2rev: 5'-TCGGGGCTTTATCTAACTCG-3'; *BCL2L*1-fwd: 5'-CCCTCCTCTCAGGAAGGTCT-3', *BCL2L*1-rev: 5'-TTTGCTCTGAATTCCCCAAA-3'; *BCL2L*2-fwd: 5'-TGCAAGTTCCCCTGTCTCTT-3', *BCL2L*2-rev: 5'-CCCCCTAGACCTTCCTGAGA-3'; *BCL2L*3-fwd: 5'-GGACGGATGAAATAGGCTGA-3', *BCL2L*3-rev: 5'-GGTAGCTTCCAGACGCAAGA-3'; *BCL2L*4-fwd: 5'-AGAGTACTCCTGGCTCCCAGT-3', *BCL2L*4-rev: 5'-GTATCACAGGTCGGGAGAGG-3'. Amplified promoter sequences were analyzed by either analytical DNA-agarose gel electrophoresis or q-PCR.

Chromatin immunoprecipitation assay

Chromatin immunoprecipitation was performed using a ChIP assay kit (Upstate Biotechnology) according to the manufacturer's instructions. We performed chromatin immunoprecipitation in cells based on the protocol provided by Upstate Biotechnology. The chromatin was prepared from 5×10^6 cells and subjected to ChIP assay as previously described [42]. 4 μg of anti-STAT3 rabbit polyclonal antibody or control rabbit IgG were used for immunoprecipitation. The following primers, 5'- ATATTATCTTATCCACATCC −3', and 5'- AACATCAGACAAACCCAAAT −3', were used to amplify the human TET3 promoter region (−1440~−1230 bp from the transcription start site), spanning the putative STATx-binding sites that contained a putative STATx-binding sites as suggested by TRANSFAC software.

Statistical analysis

At least three replicates were compiled for all experiments, and n-values listed in the figures and/or the legends. Statistical analysis was performed using GraphPad Prism 7.0 or Microsoft Excel. Data were represented as the mean ± the standard deviation. All data are normally distributed, and the variances are similar. The Student's *t* test was used to analyze whether two experimental groups have significant difference. A two-tailed value of $P < 0.05$ was considered statistically significant, while n.s. indicates not significantly different.

Supplementary Material

Refer to Web version on PubMed Central for supplementary material.

Acknowledgements

We thank the dedication of staff members at the flow cytometry core, light microscopy core, animal facility core, and pathology core as well as the DNA/RNA synthesis core facility at the Beckman Research Institute at City of Hope Comprehensive Cancer Center for their technical assistance. We thank Dr. Laurent A. Bentolila for help with STED imaging, which was performed at the California NanoSystems Institute Advanced Light Microscopy/ Spectroscopy Shared Facility at UCLA supported with funding from NSF Major Research Instrumentation grant (CHE-0722519). We also acknowledge the contribution of staff members at the animal facilities at City of Hope.

Funding

This work is funded in part by R01CA122976 and R01CA146092 (to H Yu), as well as the Billy and Audrey Wilder Endowment (to H Yu). Research reported in this publication was supported by the National Cancer Institute of the National Institutes of Health under grant number P30CA033572 (to City of Hope Comprehensive Cancer Center). The content is solely the responsibility of the authors and does not necessarily represent the official views of the National Institutes of Health.

References

1. Weaver VM, Roskelley CD. Extracellular matrix: the central regulator of cell and tissue homeostasis. Trends in cell biology 1997; 7: 40–42. [PubMed: 17708898]
2. Frantz C, Stewart KM, Weaver VM. The extracellular matrix at a glance. Journal of cell science 2010; 123: 4195–4200. [PubMed: 21123617]
3. Levental KR, Yu H, Kass L, Lakins JN, Egeblad M, Erler JT et al. Matrix crosslinking forces tumor progression by enhancing integrin signaling. Cell 2009; 139: 891–906. [PubMed: 19931152]
4. Lu P, Weaver VM, Werb Z. The extracellular matrix: a dynamic niche in cancer progression. The Journal of cell biology 2012; 196: 395–406. [PubMed: 22351925]
5. Pickup MW, Mouw JK, Weaver VM. The extracellular matrix modulates the hallmarks of cancer. EMBO reports 2014; 15: 1243–1253. [PubMed: 25381661]
6. Acerbi I, Cassereau L, Dean I, Shi Q, Au A, Park C et al. Human breast cancer invasion and aggression correlates with ECM stiffening and immune cell infiltration. Integrative biology : quantitative biosciences from nano to macro 2015; 7: 1120–1134. [PubMed: 25959051]
7. Sun Y, Chen CS, Fu J. Forcing stem cells to behave: a biophysical perspective of the cellular microenvironment. Annual review of biophysics 2012; 41: 519–542.
8. Lathia JD, Gallagher J, Heddleston JM, Wang J, Eyler CE, Macswords J et al. Integrin alpha 6 regulates glioblastoma stem cells. Cell stem cell 2010; 6: 421–432. [PubMed: 20452317]
9. Herrmann A, Cherryholmes G, Schroeder A, Phallen J, Alizadeh D, Xin H et al. TLR9 is critical for glioma stem cell maintenance and targeting. Cancer research 2014; 74: 5218–5228. [PubMed: 25047528]
10. Schroeder A, Herrmann A, Cherryholmes G, Kowolik C, Buettner R, Pal S et al. Loss of androgen receptor expression promotes a stem-like cell phenotype in prostate cancer through STAT3 signaling. Cancer research 2014; 74: 1227–1237. [PubMed: 24177177]

11. Yu H, Lee H, Herrmann A, Buettner R, Jove R. Revisiting STAT3 signalling in cancer: new and unexpected biological functions. Nature reviews Cancer 2014; 14: 736–746. [PubMed: 25342631]
12. Wang J, Wang H, Li Z, Wu Q, Lathia JD, McLendon RE et al. c-Myc is required for maintenance of glioma cancer stem cells. PloS one 2008; 3: e3769. [PubMed: 19020659]
13. Jin F, Zhao L, Zhao HY, Guo SG, Feng J, Jiang XB et al. Comparison between cells and cancer stem-like cells isolated from glioblastoma and astrocytoma on expression of anti-apoptotic and multidrug resistance-associated protein genes. Neuroscience 2008; 154: 541–550. [PubMed: 18462887]
14. Tagscherer KE, Fassl A, Campos B, Farhadi M, Kraemer A, Bock BC et al. Apoptosis-based treatment of glioblastomas with ABT-737, a novel small molecule inhibitor of Bcl-2 family proteins. Oncogene 2008; 27: 6646–6656. [PubMed: 18663354]
15. Guo JU, Su Y, Zhong C, Ming GL, Song H. Hydroxylation of 5-methylcytosine by TET1 promotes active DNA demethylation in the adult brain. Cell 2011; 145: 423–434. [PubMed: 21496894]
16. Tahiliani M, Koh KP, Shen Y, Pastor WA, Bandukwala H, Brudno Y et al. Conversion of 5-methylcytosine to 5-hydroxymethylcytosine in mammalian DNA by MLL partner TET1. Science (New York, NY 2009; 324: 930–935.
17. Veron N, Peters AH. Epigenetics: Tet proteins in the limelight. Nature 2011; 473: 293–294. [PubMed: 21593859]
18. Yang L, Yu SJ, Hong Q, Yang Y, Shao ZM. Reduced Expression of TET1, TET2, TET3 and TDG mRNAs Are Associated with Poor Prognosis of Patients with Early Breast Cancer. PloS one 2015; 10: e0133896. [PubMed: 26207381]
19. Wu MZ, Chen SF, Nieh S, Benner C, Ger LP, Jan CI et al. Hypoxia Drives Breast Tumor Malignancy through a TET-TNFalpha-p38-MAPK Signaling Axis. Cancer research 2015; 75: 3912–3924. [PubMed: 26294212]
20. Cui Q, Yang S, Ye P, Tian E, Sun G, Zhou J et al. Downregulation of TLX induces TET3 expression and inhibits glioblastoma stem cell self-renewal and tumorigenesis. Nature communications 2016; 7: 10637.
21. Cimmino L, Dawlaty MM, Ndiaye-Lobry D, Yap YS, Bakogianni S, Yu Y et al. TET1 is a tumor suppressor of hematopoietic malignancy. Nature immunology 2015; 16: 653–662. [PubMed: 25867473]
22. Huang H, Jiang X, Li Z, Li Y, Song CX, He C et al. TET1 plays an essential oncogenic role in MLL-rearranged leukemia. Proceedings of the National Academy of Sciences of the United States of America 2013; 110: 11994–11999. [PubMed: 23818607]
23. Johnson KC, Houseman EA, King JE, von Herrmann KM, Fadul CE, Christensen BC. 5-Hydroxymethylcytosine localizes to enhancer elements and is associated with survival in glioblastoma patients. Nature communications 2016; 7: 13177.
24. Takai H, Masuda K, Sato T, Sakaguchi Y, Suzuki T, Suzuki T et al. 5-Hydroxymethylcytosine plays a critical role in glioblastomagenesis by recruiting the CHTOP-methylosome complex. Cell reports 2014; 9: 48–60. [PubMed: 25284789]
25. Ito S, D'Alessio AC, Taranova OV, Hong K, Sowers LC, Zhang Y. Role of Tet proteins in 5mC to 5hmC conversion, ES-cell self-renewal and inner cell mass specification. Nature 2010; 466: 1129–1133. [PubMed: 20639862]
26. Koh KP, Yabuuchi A, Rao S, Huang Y, Cunniff K, Nardone J et al. Tet1 and Tet2 regulate 5-hydroxymethylcytosine production and cell lineage specification in mouse embryonic stem cells. Cell stem cell 2011; 8: 200–213. [PubMed: 21295276]
27. Huang Y, Chavez L, Chang X, Wang X, Pastor WA, Kang J et al. Distinct roles of the methylcytosine oxidases Tet1 and Tet2 in mouse embryonic stem cells. Proceedings of the National Academy of Sciences of the United States of America 2014; 111: 1361–1366. [PubMed: 24474761]
28. Brown CE, Starr R, Aguilar B, Shami AF, Martinez C, D'Apuzzo M et al. Stem-like tumor-initiating cells isolated from IL13Ralpha2 expressing gliomas are targeted and killed by IL13-zetakine-redirected T Cells. Clin Cancer Res 2012; 18: 2199–2209. [PubMed: 22407828]

29. Brown CE, Starr R, Martinez C, Aguilar B, D'Apuzzo M, Todorov I et al. Recognition and killing of brain tumor stem-like initiating cells by CD8+ cytolytic T cells. Cancer research 2009; 69: 8886–8893. [PubMed: 19903840]
30. Singh SK, Clarke ID, Terasaki M, Bonn VE, Hawkins C, Squire J et al. Identification of a cancer stem cell in human brain tumors. Cancer research 2003; 63: 5821–5828. [PubMed: 14522905]
31. Branco MR, Ficz G, Reik W. Uncovering the role of 5-hydroxymethylcytosine in the epigenome. Nature reviews Genetics 2012; 13: 7–13.
32. Zhang F, Liu Y, Zhang Z, Li J, Wan Y, Zhang L et al. 5-hydroxymethylcytosine loss is associated with poor prognosis for patients with WHO grade II diffuse astrocytomas. Scientific reports 2016; 6: 20882. [PubMed: 26864347]
33. Mathieu J, Zhang Z, Zhou W, Wang AJ, Heddleston JM, Pinna CM et al. HIF induces human embryonic stem cell markers in cancer cells. Cancer research 2011; 71: 4640–4652. [PubMed: 21712410]
34. Magee JA, Piskounova E, Morrison SJ. Cancer stem cells: impact, heterogeneity, and uncertainty. Cancer cell 2012; 21: 283–296. [PubMed: 22439924]
35. Meissner A, Mikkelsen TS, Gu H, Wernig M, Hanna J, Sivachenko A et al. Genome-scale DNA methylation maps of pluripotent and differentiated cells. Nature 2008; 454: 766–770. [PubMed: 18600261]
36. Meissner A Epigenetic modifications in pluripotent and differentiated cells. Nature biotechnology 2010; 28: 1079–1088.
37. Baylin SB, Jones PA. A decade of exploring the cancer epigenome - biological and translational implications. Nat Rev Cancer 2011; 11: 726–734. [PubMed: 21941284]
38. Baylin SB. Resistance, epigenetics and the cancer ecosystem. Nature medicine 2011; 17: 288–289.
39. Prasad P, Mittal SA, Chongtham J, Mohanty S, Srivastava T. Hypoxia-Mediated Epigenetic Regulation of Stemness in Brain Tumor Cells. Stem cells (Dayton, Ohio) 2017; 35: 1468–1478.
40. Jiang X, Hu C, Ferchen K, Nie J, Cui X, Chen CH et al. Targeted inhibition of STAT/TET1 axis as a therapeutic strategy for acute myeloid leukemia. Nature communications 2017; 8: 2099.
41. Hu Y, Smyth GK. ELDA: extreme limiting dilution analysis for comparing depleted and enriched populations in stem cell and other assays. Journal of immunological methods 2009; 347: 70–78. [PubMed: 19567251]
42. Herrmann A, Priceman SJ, Swiderski P, Kujawski M, Xin H, Cherryholmes GA et al. CTLA4 aptamer delivers STAT3 siRNA to tumor-associated and malignant T cells. The Journal of clinical investigation 2015; 125: 2547.

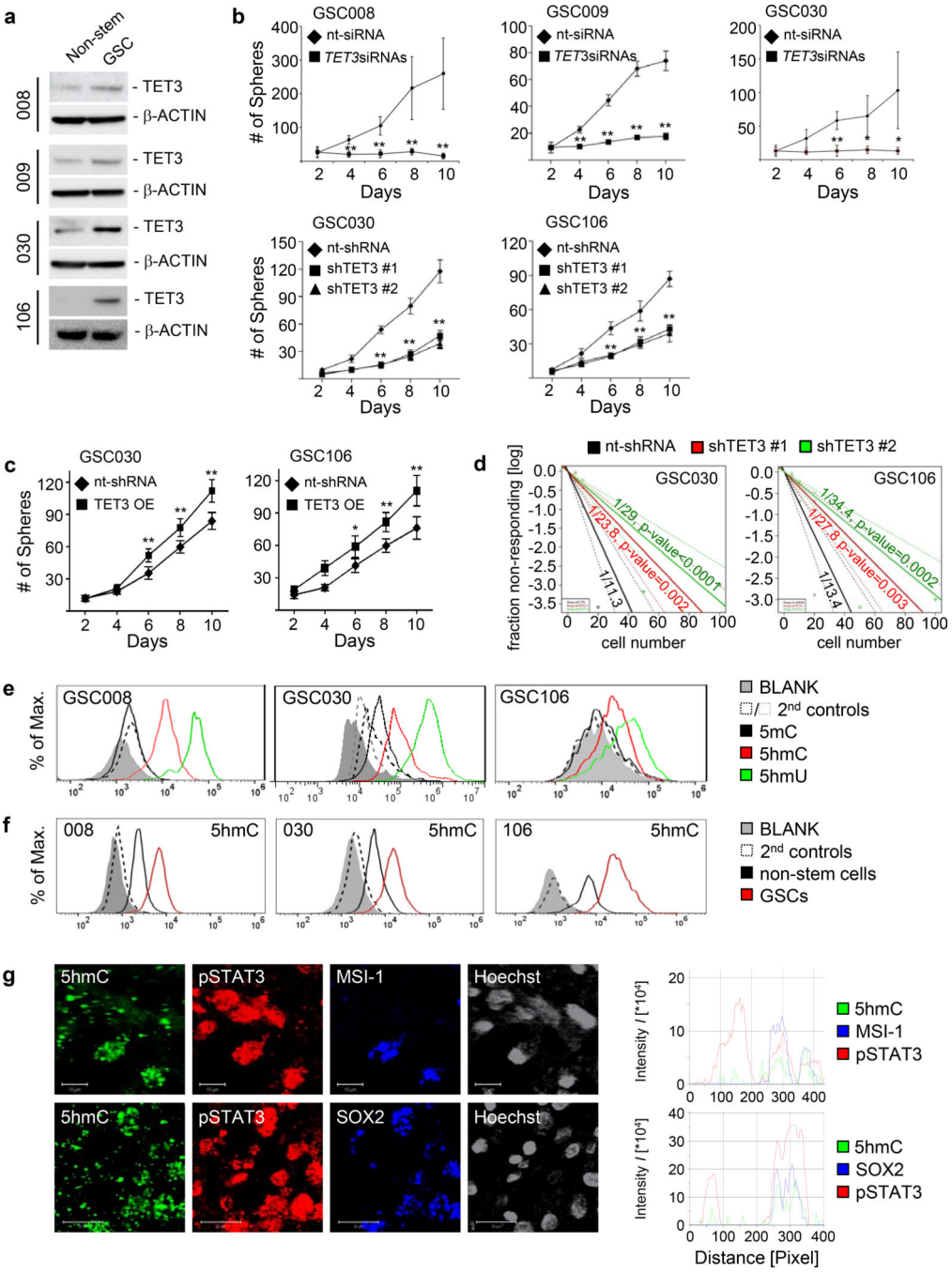

Fig. 1.

TET3 critical for characteristic tumor sphere formation is overexpressed in glioma stem cells favoring 5hmC accumulation. **a** TET3 protein expression was assessed by Western blotting compared in differentiated non-stem counterparts and primary human GSCs. Actin was re-probed and shown as a loading control. **b** Reduced tumor sphere formation by TET3 silencing was shown in primary human GSCs, GSC008, GSC009, GSC030 and GSC106. GSC008, GSC009, and GSC030 cells were treated with CpG-*luciferase*-siRNA or CpG-*TET3*-siRNAs every other day (n = 6) (upper panels). GSC030 and GSC106 were stably

transduced with non-targeting shRNA or inducible *TET3* shRNAs, and were treated with 5 μg/ml of doxycycline for shRNA induction (n = 6) (lower panels). SD shown, T-test: *) $P < 0.05$, **) $P < 0.01$, ***) $P < 0.001$. **c** Increased tumor sphere formation by TET3 overexpression was shown in primary human GSCs, GSC030 and GSC106. GSC030 and GSC106 were stably transduced with full length human TET3 cDNA (n = 6). SD shown, T-test: *) $P < 0.05$, **) $P < 0.01$. **d** Decreased tumorigenicity of primary human GSCs upon *TET3* silencing was assessed by LDA. GSCs were stably transduced with non-targeting shRNA or inducible shTET3s, and treated with 5 μg/ml of doxycycline for shRNA induction. **e** 5hmC accumulation in primary human GSCs, GSC008, GSC030, and GSC106 were confirmed by flow cytometry upon digestion of RNA species. 5hmU accumulation as a TET3 independent DNA deamination alternative to TET3 dependent 5hmC-5fC conversion was included. **f** 5hmC in GSCs were compared to their non-stem counterparts by flow cytometry. **g** 5hmC (green) accumulation restricted to $pSTAT3^{+}MSI\text{-}1^{+}$ and $pSTAT3^{+}SOX2^{+}$ GBM cells but not to single positive $pSTAT3^{+}$ GBM cells shown by confocal microscopy upon staining glioma patient tissue sections (left). Scale, 20 μm. Tissue profiles showing 5hmC accumulation confined to GSC-$marker^{+}$ cells (right). **a-g** Representative data from 3 independent experiments are shown.

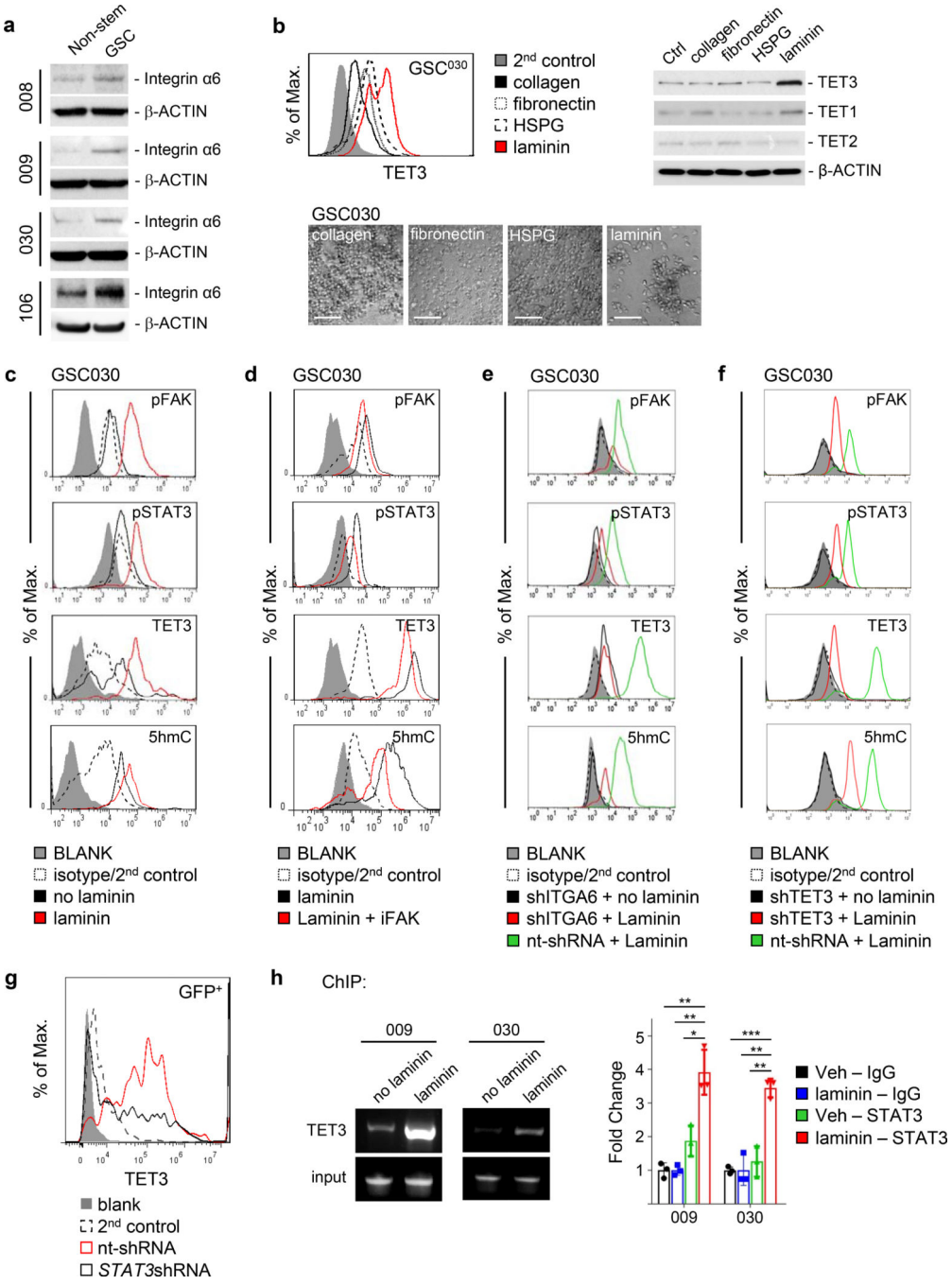

Fig. 2.

Integrin α6/FAK signaling feeds STAT3 dependent TET3 expression and 5hmC accumulation. **a** Integrin α6 protein expressions in GSCs were compared to those of differentiated non-stem counterparts by Western blotting. Actin was re-probed and shown as a loading control. **b** Integrin α6 signaling mediated TET3 expression was assessed by flow cytometry and Western blotting in primary human stem-like GSC030 upon engagement with laminin compared to other components of the ECM (upper panels). Characteristic sphere formation upon exposure of a GSC single cell suspension to laminin and other ECM

components is shown by bright field microscopy (lower panels). Scale, 100 μm. **c** Ectopic stimulation of stem-like GSC030 with laminin triggers activation of FAK/STAT3, expression of TET3 and 5hmC accumulation as shown by flow cytometry (top to bottom). **d** Blocking FAK activity with FAK inhibitor during stimulation of GSCs with laminin reduced activation of FAK/STAT3, expression of TET3 and 5hmC accumulation as shown by flow cytometry (top to bottom). **e** Silencing integrin α6 with inducible shRNA during stimulation of GSCs with laminin reduced activation of FAK/STAT3, expression of TET3 and 5hmC accumulation as shown by flow cytometry (top to bottom).**f** Silencing TET3 with inducible shRNA during stimulation of GSCs with laminin reduces activation of FAK/STAT3, expression of TET3 and 5hmC accumulation as shown by flow cytometry (top to bottom). **g** STAT3 silencing reducing TET3 expression was confirmed *in vivo* using human glioma U251 cells. GFP expression was controlled by the *SOX2* promoter. GFP^+ glioma cells considered stem-like phenocopies were analyzed for TET3 expression by flow cytometry once tumors were dissected and a single cell suspension was prepared. **h** STAT3 contributing to TET3 expression was validated by ChIP assay in two independent primary human GSCs, GSC009 and GSC030, and quantified. SD shown, T-test: *) $P < 0.01$, **) $P < 0.01$, **) $P < 0.001$. **a-h** Representative data from 3 independent experiments are shown.

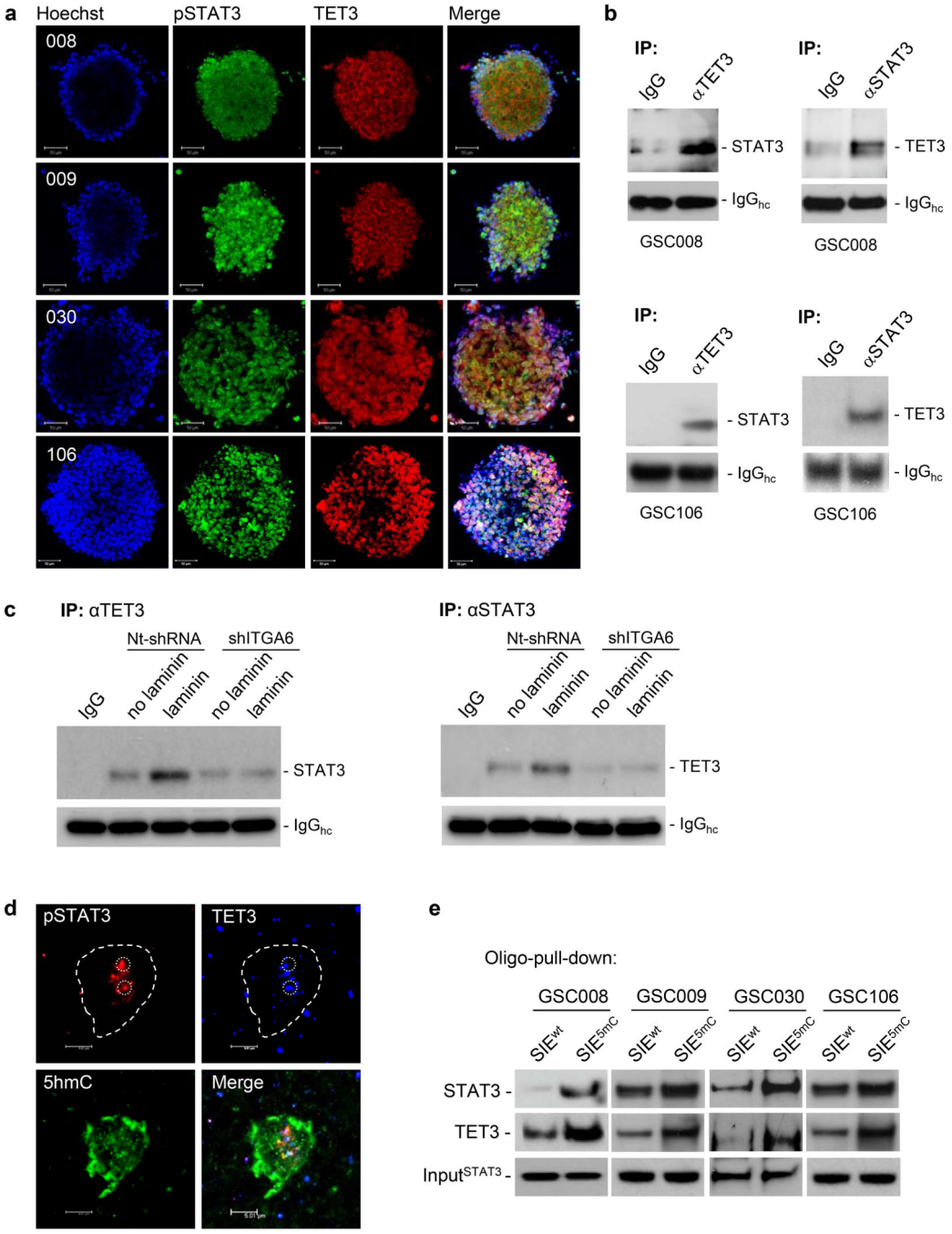

Fig. 3.

STAT3 and TET3 physically interact and cooperate in binding to methylated STAT3 target DNA sequences. **a** STAT3 and TET3 subcellular co-localization was assessed in four independent primary human GSC lines GSC008, GSC009, GSC030, and GSC106 by confocal microscopy. Scale, 50 μm. **b** Physical interaction of STAT3 and TET3 was shown by co-IP pulling down TET3 and detecting STAT3 and vice versa using whole cell lysates prepared from primary human GSCs, GSC030 and GSC106. **c** Physical interaction of STAT3 and TET3 was reduced by silencing integrin α6 with inducible shITGA6 as shown

by co-IP pulling down TET3 and detecting STAT3 and vice versa using whole cell lysates prepared from primary human GSC106. **d** Nuclear co-localization of activated pY^{705}STAT3 with TET3 and 5hmC was assessed by confocal STED microscopy in glioma patient tissue. Scale, 5 μm. **e** Enhanced cooperative binding of STAT3 and TET3 to methylated STAT3 target DNA sequence (SIE^{5mC}) was shown by oligo-pull-down assay using unmethylated or methylated SIE oligo. Protein complexes were detected in Western blot procedure after electrophoretic protein separation on SDS-PAGE. **a-e** Representative data from 3 independent experiments are shown.

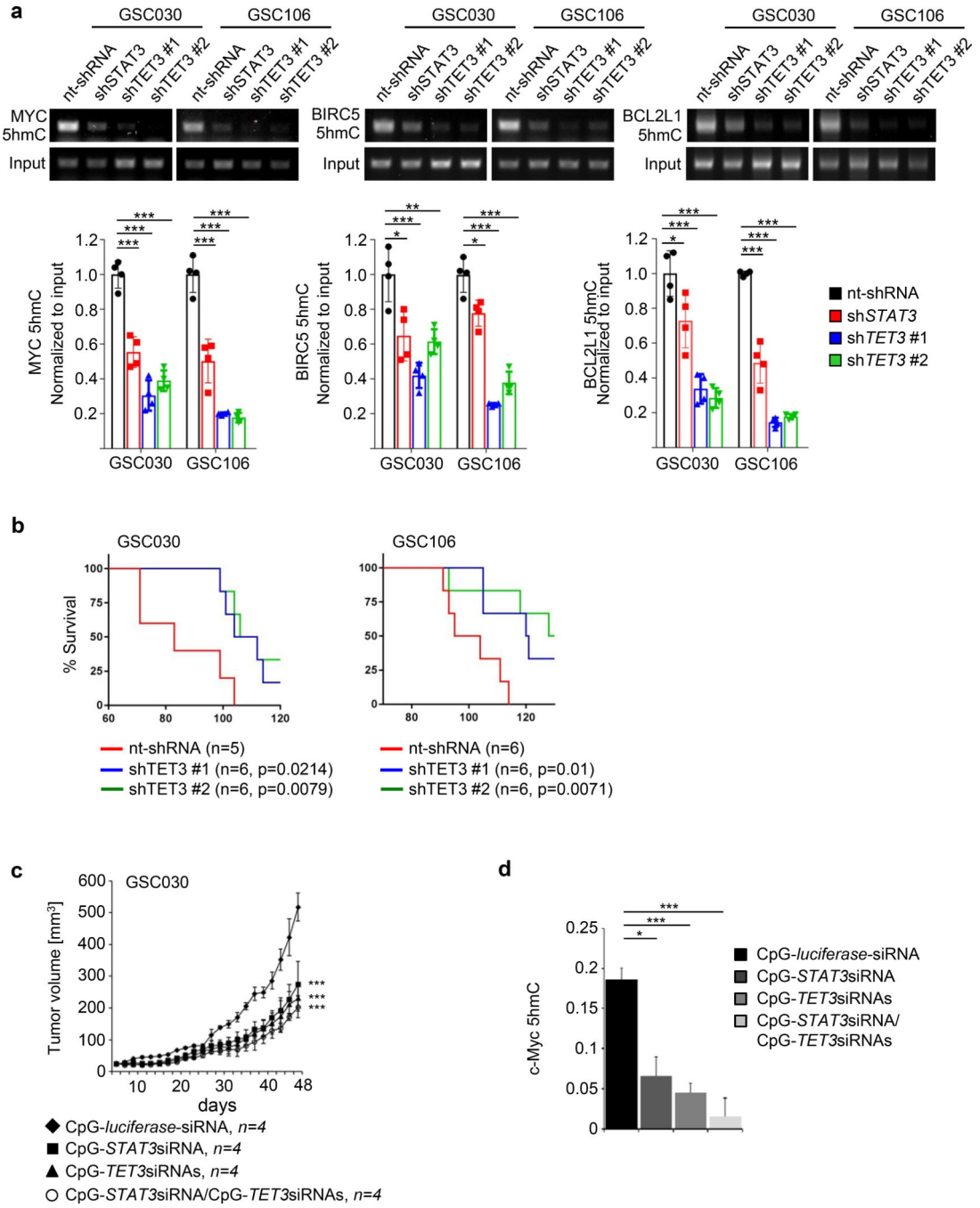

Fig. 4.

STAT3 contributes to oncogene promoter hydroxymethylation in GSCs *in vitro* and STAT3 or TET3 knockdown prolongs mouse survival *in vivo*. **a** Hydroxymetylation of oncogene promoters upon STAT3 knockdown (*shSTAT3*) or TET3 knockdown (*shTET3*) was assessed by PCR using mRNA harvested from human primary GSCs, GSC030 and GSC106. Amplified cDNA was treated to sensitize non-hydroxymethylated cDNA for restriction enzyme digestion and products were separated on DNA gel (upper panels). Decreased oncogene promoter hydroxymetylation upon STAT3 knockdown was quantified by qPCR

(lower panels). SD shown; T-test: *) $P < 0.05$, **) $P < 0.01$, ***) $P < 0.001$. Representative data from 3 independent experiments are shown. **b** Tumors grown from primary human GSCs stably expressing non-targeting shRNA or inducible *shTET3* were treated with 2 mg/ml doxycycline water. Mouse survival was plotted out by Kaplan-Meier survival curves. **c** Tumors grown from primary human GSC, GSC030 were treated with CpG-siRNA conjugates as indicated including control CpG-*luciferase*-siRNA. Tumor growth kinetics were assessed. SD shown; T-test: ***) $P < 0.001$. **d** STAT3 and TET3 sensitive c-Myc oncogene promoter hydroxymetylation of GSC tumors treated as indicated was determined upon isolation of gDNA and treatment of gDNA to sensitize non-hydroxymethylated cDNA for restriction enzyme digestion. SD shown; T-test: *) $P < 0.05$, ***) $P < 0.001$.

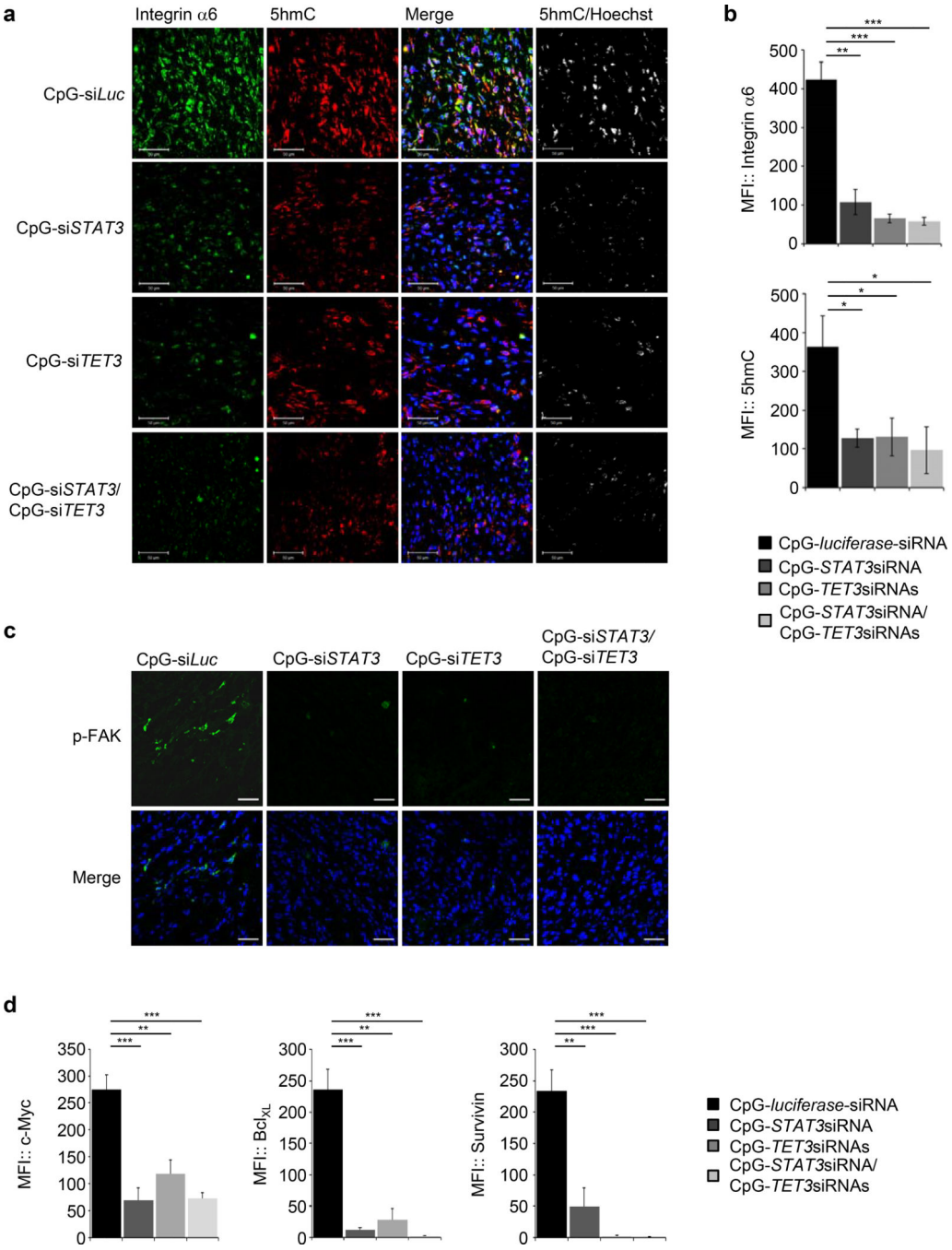

Fig. 5.

STAT3 critically contributes to oncogene promoter hydroxymethylation in GSCs *in vivo*. **a** STAT3- and TET3-sensitive protein expressions of integrin α6 as well as 5hmC accumulation in GSC tumors treated as indicated were assessed by confocal microscopy and **b** quantified. Scale, 50 μm. SD shown; T-test: *) $P < 0.05$, **) $P < 0.01$, ***) $P < 0.001$. **c** FAK protein expression in GSC tumors treated as indicated were assessed by confocal microscopy. Scale, 50 μm. **d** Reduced oncogene expression upon treatment of GSC tumors

as indicated as determined by confocal microscopy and quantified. SD shown; T-test: **) $P < 0.01$, ***) $P < 0.001$.

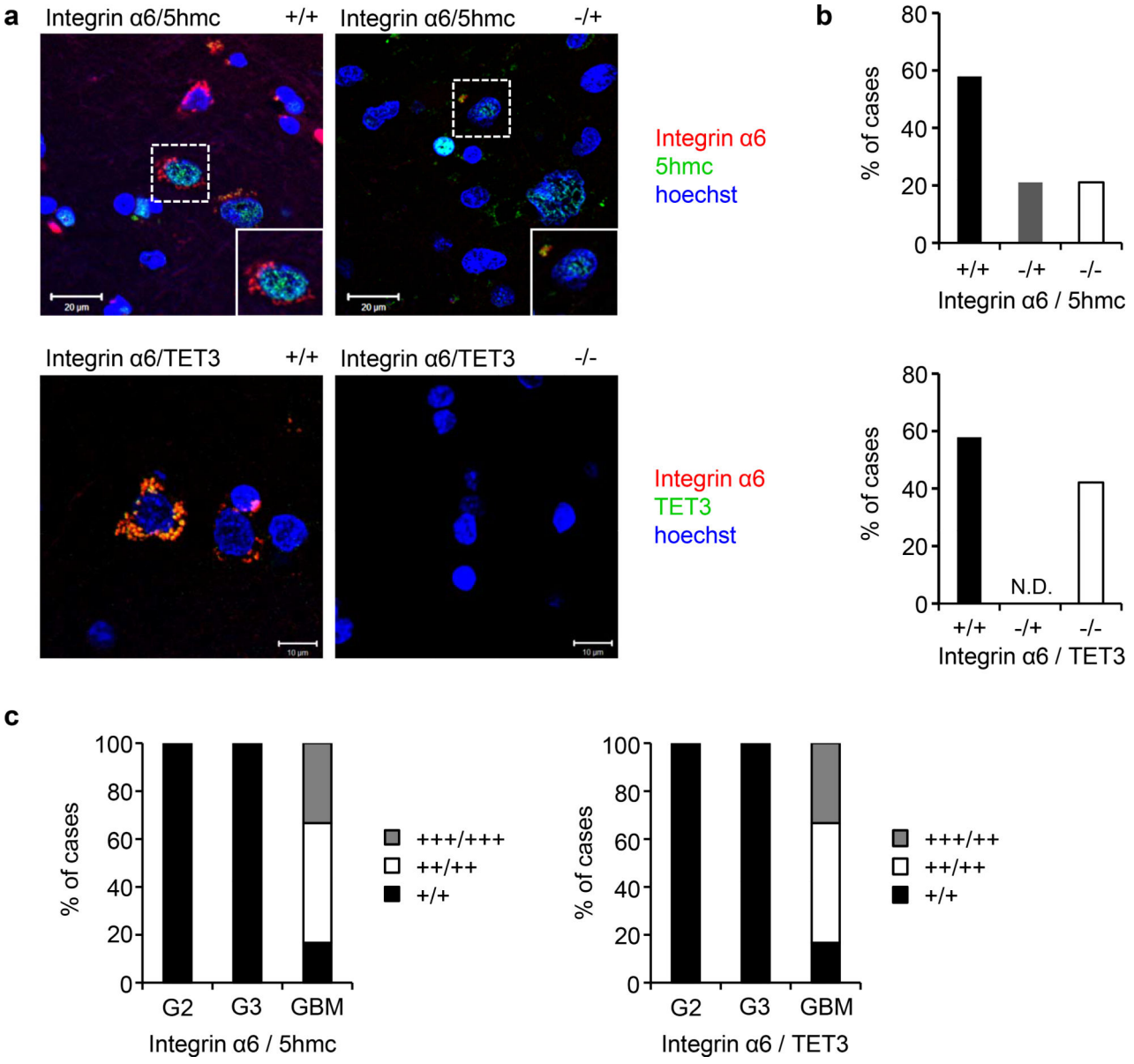

Fig. 6.

Integrin α6 and TET3 expression resulting in 5hmC accumulation is confined to high grade glioma. **a** Integrin α6 and 5hmC (upper panels) or TET3 (lower panels) expression was assessed by immunohistochemistry followed by confocal microscopy of human brain tumor patient biopsies. Scale 20 μm (upper panels) and 10 μm (lower panels). **b** Quantitative case distribution of integrin α6/5hmC (upper panels) or integrin α6/TET3 (lower panels) expression. A total of 19 brain tumor cases were analyzed. **c** High frequency occurrence of integrin α6+/5hmC+ (left panel) or integrin α6+/TET3+ (right panel) expression is restricted to high grade glioblastoma as assessed from 19 brain tumor cases analyzed. **a-c** Total 19 patient cases were analyzed, and 5 to 10 images were acquired per slide.